Effect of metal precursor on Cu/ZnO/Al_2O_3 synthesized by flame spray pyrolysis for direct DME production

Seungcheol Lee[1], Katja Schneider[2], Julia Schumann[3], Aswani K. Mogalicherla[1], Peter Pfeifer[2], Roland Dittmeyer[1, 2]

[1]Institute of Catalysis Research and Technology, Karlsruhe Institute of Technology, Eggenstein-Leopoldshafen, Germany

[2]Institute for Micro Process Engineering, Karlsruhe Institute of Technology, Eggenstein-Leopoldshafen, Germany

[3]Department of Inorganic Chemistry, Fritz-Haber-Institut der Max-Planck-Gesellschaft, Berlin, Germany

1. Introduction

Current energy carriers like fossil petroleum, coal, and natural gas need to be substituted in the long term with sustainable energy carriers due to their depletion and environmental pollution. Dimethyl ether (DME) produced from biomass (or stranded natural gas) has received much attention as a promising fuel for the near future due to its clean combustion properties and wide applicability. DME can be used as an LPG (liquefied petroleum gas) alternative and serves as a raw material for hydrocarbons, dimethyl sulfate and methyl acetate [1-3]. Comparing with diesel as a transportation fuel, DME is advantageous in terms of performance and environmental friendliness. DME combustion emits less carbon dioxide and soot than diesel combustion. In addition, the efficiency for transformation of chemical energy into motion is better than for diesel.

DME can be produced from syngas in a two-step process via methanol synthesis and methanol dehydration in two separate catalytic reactors, or in a one-step process, direct DME synthesis, where both reactions are carried out in one reactor on a hybrid or bifunctional catalyst. The one-step process is preferred in terms of thermodynamic limitation of the syngas conversion [4, 5]. The main reactions in direct DME synthesis are:

$$CO + 2H_2 \rightleftharpoons CH_3OH \quad (1)$$

$$CO_2 + 3H_2 \rightleftharpoons CH_3OH + H_2O \quad (2)$$

$$2CH_3OH \rightleftharpoons DME + H_2O \quad (3)$$

$$CO + H_2O \rightleftharpoons CO_2 + H_2 \quad (4)$$

Methanol is synthesized from syngas, a mixture of CO_2, CO and H_2 according equation (1) and (2). As the produced methanol is consumed to form DME by the dehydration (3), the equilibrium of methanol synthesis shifts and syngas can be converted to a higher extent. By the water-gas shift reaction (4), water

is converted to CO_2 and H_2. Copper-based catalysts ($Cu/ZnO/Al_2O_3$) and solid acids (γ-alumina and ZSM-5) have been used for methanol synthesis and methanol dehydration respectively.

The methanol production from syngas started in the early twentieth century and catalysts have been developed. The $Cu/ZnO/Al_2O_3$ has been established widely in industry due to high activity and selectivity as well as the low mass specific costs compared to noble metals. Nevertheless, intrinsic reaction mechanism and active sites have been under debate. Pure copper can produce methanol, but deactivation takes place rapidly by the sintering of copper particles [6, 7]. Several reports give hints to prove these matters. Presence of ZnO and Al_2O_3 can promote the copper catalytic activity and prevent the copper sintering [8-10]. The structure and composition of those metal and metal oxides mixtures are strongly related to the catalytic activity, so that the synthesis and post treatments need to be carefully controlled.

The co-precipitation method by using metal nitrates has been used commonly for the $Cu/ZnO/Al_2O_3$ catalyst. This method is very sensitive towards the final catalyst behavior by its synthesis parameters such as synthesis temperature, synthesis pH and calcination temperature. The activity is easily influenced by a small change of these parameters [11]. Hence the enhancement of the reproducibility and scale-up of the synthesis are difficult and it is worthy to explore other ways. That became a motivation to study the synthesis of the $Cu/ZnO/Al_2O_3$ by flame spray pyrolysis (FSP) as a more reproducible and simpler synthesis method [12].

Flame synthesis of fine particles was initially developed for ceramics production. However, there is possibility for extending similar technology for a large scale production of catalyst nanoparticles [13]. FSP is one possibility within the flame synthesis of fine particles. It uses a liquid, flammable solvent and typically also flammable metal precursors. The metal precursors need to be dissolved in flammable solvents and the mixture is sprayed along with oxygen (air) or methane/oxygen (air) as feed into a flame. The metal precursors are decomposed in the high temperature flame (up to 2000 ^oC) into gaseous metal ions. They subsequently nucleate to form particles. By coalescence and aggregation, the particles grow up in size. The process conditions such as the flame temperature and the residence time in the flame determine the particle size and crystal structure [14]. This technique has been used for single metal oxides and frequently also for multi-component metal oxide particle systems [14].

A few research groups have recently reported $Cu/ZnO/Al_2O_3$ particle synthesis via flame synthesis. Jensen et al. reported the $Cu/ZnO/Al_2O_3$ by flame combustion synthesis using vapor phase metal precursors (aerosol technique); these catalysts have been well characterized and were applied in methanol synthesis [15]. Huber et al. and Ahmad et al. showed catalytic applications of the flame synthesized $Cu/ZnO/Al_2O_3$ with liquid metal precursors in the water-gas shift reaction and DME synthesis [16, 17], respectively.

Although FSP can offer high surface area and easy doping of catalysts, employing organometallic precursors is limited in an industrial scale due to safety issues and costs. For example, Kam et al. demonstrated advantages in doping of another element, La, on the Cu/ZnO by FSP [18]. They could

enhance the activity of the catalyst by the FSP technique, but did not overcome applying expensive organometallic precursors. According to all former reports, FSP can provide similar, or even better, physicochemical and catalytic properties of copper catalysts compared to the conventional precipitated catalysts. In order to be industrially applicable, more detailed studies are required for the FSP technology such as reducing the precursor and solvent cost.

Therefore, we employed also metal nitrates as metal precursor and ethanol as solvent for synthesis of $Cu/ZnO/Al_2O_3$ catalyst. The catalytic activity comparison between metal nitrate and organometallic precursor derived catalysts was investigated on direct DME synthesis in a tubular fixed-bed reactor. We further varied the Cu/Zn ratio as well.

2. Experimental

2.1. Catalyst synthesis by FSP

Two general types of metal precursors were applied to synthesize $Cu/ZnO/Al_2O_3$ (CZA) catalysts by FSP; one type was based on nitrate precursors, the other was based on organometallic compounds. The nitrate based precursor solutions (nitrate type) were prepared by mixing copper (II) nitrate tri-hydrate (Sigma-Aldrich, >99 %), zinc nitrate hexa-hydrate (Sigma-Aldrich, >99 %) and aluminum nitrate nona-hydrate (ChemPur, 98.5 %) in ethanol. Different molar ratios of copper, zinc and aluminum were prepared (Cu:Zn:Al = 5:4:1, 6:3:1 and 7:2:1) and are abbreviated as 5Cu4Zn1An-nitrate, 6Cu3Zn1Al-nitrate and 7Cu2Zn1Al-nitrate respectively. The organometallic precursor solutions (organometallic type) were prepared with copper bis-2-ethylhexanoate (Alfa Aesar, 98 %), zinc bis-2-ethylhexanoate (Alfa Aesar, 80 % in mineral spirits) and aluminum sec-butoxide (Alfa Aesar, 97 %), and a di-methylformamide (DMF)/xylene mixture (volume ratio = 1/1) was used as a solvent. Also the same three different molar ratios were prepared for organometallic type samples, and are abbreviated as 4Cu4Zn1Al-organo, 6Cu3Zn1Al-organo and 7Cu2Zn1Al-organo. The total molar concentration of the metal precursors in all solutions was set to 0.5 M.

A flame generator (NanoPowderNozzle®) and collection cylinder purchased from Tethis were set up in a fume hood. The scheme of the flame generator used for this study is shown in Figure 1. The flame was fed by CH_4 and O_2 mixture with a flow rate of 0.5 L/min and 1.9 L/min, respectively. The metal precursor solution was fed to the flame with a flow rate of 5 ml/min by a syringe pump (PHD Ultra™, Harvard). Additional dispersion gas (O_2) was fed through the gap around the precursor solution nozzle (feed rate: 3.5 L/min, pressure: 2 bar). In order to stabilize the flame, the sheath gas (O_2) was fed around the flame with 5 L/min flow rate. A vacuum pump facilitated particles deposition on a glass fiber filter on top of the collection cylinder. The deposited particles were scratched carefully from the filter after cooling down the FSP system.

Figure 1 here

2.2. Synthesis of ZSM-5

In the present work, the dehydration catalyst ZSM-5 was admixed to methanol synthesis catalyst produced from FSP. For synthesizing ZSM-5, sodium hydroxide and the template TPAOH (tetra-propylammonium hydroxide, Sigma-Aldrich, 1.0 M in water) were initially dissolved in water. TEOS (tetra-ethylorthosilicate, Sigma-Aldrich, > 99 %) as a silica source was added to the template solution under stirring. After stirring the mixture for 2 hours, aluminum nitrate nona-hydrate (ChemPur, 98.5 %) was added under vigorous stirring. The final molar ratio was 1 TPAOH: 21 TEOS: 3 NaOH: 987 H_2O: 0.105 Al_2O_3. The solution was transferred to an autoclave vessel for the hydrothermal treatment. The autoclave was put into a preheated oven at 170 ^oC and kept there for 24 hours. After the hydrothermal treatment, the obtained white powder was collected by filtration and washed with plenty of water to remove residual reagents. The powder was dried at 80 ^oC and calcined at 550 ^oC to remove the template. The calcination in the ZSM-5 synthesis process was carried out with 1.2 ^oC/min heating ramp and 10 hours holding time at the final temperature. Afterwards the natural cooling down to room temperature in the furnace without any control was performed. For the ion-exchange, the obtained Na-ZSM-5 was put into the 0.5 M aqueous NH_4Cl solution at 70 ^oC under stirring for 24 hours. By filtration and washing with water, excess ions were removed and H-ZSM-5 was finally obtained after the calcination in the above mentioned process.

2.3. Characterization

X-ray diffraction (XRD) of the catalysts was performed with an X´Pert Pro MPD (PANalytical). Diffraction data was obtained by exposing to Cu-Kα X-ray radiation. The identification of peaks was done by the X'pert High Score software.

The reducibility of the catalysts was investigated by temperature programmed reduction (TPR). In order to perform the TPR, the catalysts were pretreated in the same way as for reaction experiments; the primary catalyst particles were pelletized, pellets were grinded and the grinded powders were sieved to obtain a particle size distribution of 50-100 μm (agglomeration diameter). The sieved powder was then put in a quartz cell of a ChemBET TPR/TPD equipment (Quantachrome). The catalyst was pretreated under a He flow at 200 ^oC. Finally, the reducibility of the sample was investigated in a flow of a H_2/Ar mixture (5 vol. % H_2) with a heating rate of 1 ^oC/min and a final ramp temperature of 400 ^oC.

BET surface area and pore size distribution were measured in an Autosorb1 machine (Quantachrome). Before the measurement, the sample was degassed at 250 ^oC.

Particle morphology and size were investigated transmission electron microscopy (TEM) and elemental analysis (EDX) was performed to identify elemental components.

By N_2O-reactive frontal chromatography [19] the N_2O chemisorption capacity of the copper catalysts has been determined. Approximately 100 mg of calcined sample (agglomerated to 50-100 µm in diameter) were placed in a fixed bed reactor. After in-situ reduction to 250 °C in 5% H_2 in Ar, the sample was cooled down to room temperature in the reducing gas, purged in He and then analyzed with a flow rate of 10 mL/min of a 1 % N_2O in He mixture at 24 °C. The N_2O chemisorption capacity was determined from the MS signal of the N_2 trace (m/z =28). On the assumption that N_2O reacts only with the surface copper atoms in a stoichiometry of $N_2O + 2Cu \rightarrow Cu_2O + N_2$ the copper surface area was calculated.

2.4. Direct DME synthesis

Direct DME synthesis over the FSP synthesized catalysts and H-ZSM-5 was carried out in a stainless steel tubular reactor. The reactor was 18 cm long and the inner diameter 8 mm. The particle size of the CZA and H-ZSM-5 was 50 - 100 µm in diameter, as described in the section 2.3. After pelletizing, grinding and sieving, the both catalysts were mechanically mixed in 1:1 weight ratio. The catalyst mixture was reduced in the reactor in a 3 vol. % H_2/N_2 mixture and heated up to 230 ^oC with 0.1 ^oC/min heating ramp. At this temperature was sustained for 8 hours. The subsequent reduction was continuously performed with pure H_2 and the temperature was increased up to 250 ^oC with 0.5 ^oC/min. After keeping the catalyst reduction at this temperature for 5 hours, the catalyst was cooled down to 100 ^oC. The reaction was carried out with the reactants, H_2, CO and CO_2. N_2 was used as an internal standard. The volumetric percentages of the gases were H_2 57.6 %, CO 28.8 %, CO_2 3.6 % and N_2 10 %. The reaction temperature range was 215 - 260 ^oC and the reaction pressure was set to 40 - 10 bar. The reactants and the products were analyzed with a gas chromatograph 7890A (Agilent Technologies) equipped with a methanation unit, a thermal conductivity detector (TCD) and a flame ionization detector (FID). Two columns, HP-Plot Q (30 m x 0.530 mm x 40.00 µm) and HP-Molesieve (5 m x 0.530 mm x 25.00 µm), could separate all gas components. CO conversion (X_{CO}) was calculated based on the molar flow rate of CO in the inlet ($\dot{N}_{CO_o}$) and outlet ($\dot{N}_{CO}$):

$$X_{CO} = (\dot{N}_{CO_o} - \dot{N}_{CO}) / \dot{N}_{CO_o} \quad (5)$$

DME selectivity (S_{DME}) and yield (Y_{DME}) were calculated based on the conversion of CO to DME:

$$S_{DME} = 2\dot{N}_{DME} / (\dot{N}_{CO_o} - \dot{N}_{CO}) \quad (6)$$

$$Y_{DME} = X_{CO} \times S_{DME} \quad (7)$$

$\dot{N}_{DME}$ is the molar flow of DME in the outlet.

3. Results and discussion

The flames generated by the both precursor types are shown in Figure 2. Each precursor type gave different figure of flames. The greenish color of the flames of the both precursors is due to the copper. Injection of the organometallic type gave more intense and unsteady flames compared to the nitrate type. DMF/xylene mixture has a lower heating value of 31.1 MJ/L. Ethanol possesses a lower heating value of 23.5 MJ/L. Organometallic precursors possess higher combustion enthalpy than nitrate precursors. Thus, the same volumetric injection of the organometallic type precursor solution provides more energy for the flame. This leads the difference of heat release between these precursors. Consequently it becomes one of the reasons for the difference in flame height. From the pictures it can be known that the organometallic precursor solution generated a taller flame. The change of metal ratio in the same precursor type did not give visible difference in flame color and height. Thus, it can be concluded that the solvent heating value was a main reason for the difference in the flame height.

Figure 2. here

The TEM analysis was used to investigate the FSP particle morphology and size. The TEM images of the CZA catalyst prepared from both precursor types are shown in Figure 3 (on the example of one molar ratio). The both types could give nanoparticles and most of them were in the nanometer size range (Figure 3. (c) and (d)). However, also some relatively large spherical particles were found (Figure 3. (a) and (b)). The EDX analysis revealed that the small particles consisted of only copper and zinc oxides whereas the big particles consisted almost exclusively of aluminum oxide. The small particles located on the big particles were also copper and zinc species without aluminum. The former studies about the flame synthesis process of $Cu/ZnO/Al_2O_3$ [15] indicated that zinc aluminate and copper aluminate spinel were formed at high temperature (>1300 ^{o}C). Formation of copper or zinc oxides was favorable at lower temperature. In the present work, we could not fully exclude spinel formation but we assumed that aluminate or aluminum oxide forms prior the zinc and copper species and aggregated to a big cluster. As the aluminum fraction in the precursor mixtures was the smallest amongst the metals, only a few of the big clusters could be found in the TEM image. Most of copper and zinc oxide clusters existed separately from the big clusters.

Figure 3. here

The particle size was measured piecewise from TEM images. The identified copper and zinc oxide particles from the both nitrate type and organometallic type systems were nearly the same in size. The particle sintering rate was reported to be proportional to the residence time [13]. The mean particle sizes of the both 6Cu3Zn1Al-nitrate and 6Cu3Zn1Al-organo were 8.91 and 9.55 nm respectively. As shown in

Figure 4, the size distributions of the both catalysts were quite similar. From this observation, it can be known that the effect of the precursor selection on size is minor at least in this case even if different metal precursors and solvent were used. The residence time is one of the greatest effects on the particle size so that the residence time difference of the both precursor system was not significant.

Figure 4. here (particle size distribution)

The crystal structure of the catalysts was investigated by XRD. The XRD patterns of the 6Cu3Zn1Al-nitrate and 6Cu3Zn1Al-organo are shown in Figure 5. The both samples possess diffraction patterns of copper oxide, zinc oxide and aluminum oxide. According to the previous reports [15, 17], the CZA synthesized by the flame technique gives broadened peaks by the dispersion of the different crystal phases. Only copper oxide was identified in their reports and other oxides could not be observed due to lower contents than copper. In this work, however, all metal oxides were well identified by XRD analysis, which means that each metal oxide is at least partially crystalline. The peaks for Al_2O_3 were found, although the aluminum content was low and the molar ratio was only 10 %. The 6Cu3Zn1Al-nitrate showed more intense Al_2O_3 peaks than the 6Cu3Zn1Al-organo in spite of equal molar fraction of aluminum in the precursor mixture. The peaks for zinc oxide were also more intense for the 6Cu3Zn1Al-nitrate. As the intensity difference correlates to surface morphology and structure of metal oxides [20], the nanostructure of the copper surface and its interaction with other metal oxide are related to the activity in reactions. These two catalysts should possess different catalytic activity.

The effect of the copper and zinc ratio on the crystal structure was also investigated for each precursor type via XRD. As shown in Figure 6, an increase of Cu/Zn ratio generally led to more intense peaks assigned to CuO and to a reduction of the peaks for ZnO. Interestingly, the peak for CuO at 39.0 (2 theta degree) was reduced at the nitrate type catalysts by increasing the Cu/Zn ratio. The peaks for Al_2O_3 were more intense while increasing the Cu/Zn ratio for both precursor types. This was more noticeable in the nitrate type than the organometallic type. Although the amount of aluminum compound was kept equally in all samples, the crystal shape and morphology could be affected by the composition of the other elements. As mentioned in a former report, it can also influence the catalytic activity [10].

Figure 5. here

Figure 6. here

For methanol synthesis and consequently for direct DME synthesis, copper oxide should be easily reducible to metallic copper. Hence, the reducibility of the catalyst was investigated by TPR. Figure 7 shows TPR spectra of all catalysts. For all the compositions, the nitrate type catalysts showed lower

reduction temperatures than the organometallic type catalysts. Some shoulder peaks were eventually assigned to the reduction process of Cu^{2+} to Cu^{1+} and then to Cu^0 in the main peak. All catalysts except for the 7Cu2Zn1Al-organo possessed a maximum in the reduction temperature well below 300 ^oC; above this temperature, copper sintering would occur quite fast if such temperature is required for reduction. The maximum reduction temperature was increased by the increase of the copper content. It is ascribed to that more copper loading produces a bulk-like copper oxide. Therefore, the dispersion of copper oxide is lower as the reduction temperature is higher [21].

Figure 7. here

Table 1. here

Further investigation of the BET surface area and exposed copper surface area was performed. The measured values of the nitrate type and organometallic type are shown in Table 1. The catalyst prepared from organometallic precursors has a little higher BET surface area. As mentioned above, the selection of precursor did not affect the particle size distribution. However, the particle morphology of multi-metallic particle was influenced by the precursor. It has been reported in literature that nitrate metal precursors and ethanol are not favorable; due to the presence of water in the flame, the particle homogeneity and particle size distribution may be poor [13]. That is in line with our observation that the nitrate type has a lower surface area than the organometallic type. When the Cu/Zn ratio was altered, the surface area was also changed. The highest value was observed with Cu/Zn/Al=6/3/1 for both precursor type.

The copper surface area was measured by N_2O-adsorption analysis. As given in the Table 1, the result of the copper surface area was opposite to the BET surface area. The organometallic type prevailed in the BET surface area, but not in the copper surface area. The 6Cu3Zn1Al-nitrate showed the highest copper surface area. It has the most exposed copper sites among them. Although the both 6Cu3Zn1Al-nitrate and 6Cu3Zn1Al-organo were synthesized with the same starting Cu/Zn ratio, by the selection of precursor the amount of copper sites was found to be much different. Therefore, a higher catalytic activity with the 6Cu3Zn1Al-nitrate would be expected. This is in line with the results of the TPR measurement, where lower reduction temperatures were observed for the nitrate type catalysts, and lower reduction temperatures are usually indicating a higher dispersion of the copper species. For sake of completeness, the determined copper amount of the 6Cu3Zn1Al-nitrate and 6Cu3Zn1Al-organo from TPR is given also in Table 1. The mass fraction of copper was relatively close to the nominal copper-to-metals ratio in the precursor solutions.

Figure 8. here

Figure 9. here

The activity of each type of catalyst for direct DME synthesis was tested in a tubular fixed-bed reactor. As predicted from the characterizations, the nitrate and organometallic type revealed different activity in direct DME synthesis reaction. As shown in Figure 8, the CO conversion increased for both catalysts with the reaction temperature. The 6Cu3Zn1Al-nitrate exhibited superior catalytic activity and the CO conversion could reach the thermodynamic equilibrium at 260 ^{o}C. The 6Cu3Zn1Al-organo showed lower activity with the pre-defined reduction protocol. According to the TPR study, the reduction temperature of the 6Cu3Zn1Al-organo was between 250 and 300 ^{o}C. Hence, an additional reaction experiment was carried out after extending the temperature ramp of the in-situ reduction to the highest temperature of 300 °C for the catalyst, but no obvious change in the conversion or selectivity was observed. The 6Cu3Zn1Al-organo system has intrinsically a low activity. The catalyst having higher copper surface area showed higher activity than the one having higher total surface area and lower copper surface area. Hence, the control of the surface area of the active copper sites is very crucial. One commercial CZA catalyst was tested as a reference. At the same reaction condition the commercial catalyst gave higher CO conversion than FSP synthesized catalyst. At 245 ^{o}C, the CO conversion reached the equilibrium.

There was no big difference in selectivity between the 6Cu3Zn1Al-nitrate and 6Cu3Zn1Al-organo as shown in Figure 9. The catalyst mixture with the 6Cu3Zn1Al-nitrate produced a little more DME and less side products: CO_2, CH_4 and other hydrocarbons. Methanol was only detected along with the 6Cu3Zn1Al-nitrate catalyst. The commercial catalyst showed a similar product distribution as the 6Cu3Zn1Al-nitrate. The CZA and H-ZSM-5 were mechanically mixed so that some produced methanol could pass the H-ZSM-5 in case of high activity of the CZA catalyst. In the case of the 6Cu3Zn1Al-organo, the overall activity was so low, that methanol could be completely converted over the H-ZSM-5 to DME and the sequential side products. As shown in Figure 10, the selectivity for DME increased with reaction temperature, and the CO_2 selectivity was influenced slightly by the reaction temperature. The selectivity is strongly related to the activity of the dehydration catalyst [22]. The produced methanol can mainly be converted to DME since the H-ZSM-5 can give high conversion of methanol to DME at similar reaction conditions [23].

Figure. 10 here

Figure. 11 here

The influence of Cu/Zn ratio was investigated on the nitrate type catalysts. Figure 11 shows the activity of the three different nitrate type catalysts. The 6Cu3Zn1Al-nitrate was the most active for converting CO. The 5Cu4Zn1Al-nitrate had the lowest copper reduction temperature, but the catalytic activity was lower than the 6Cu3Zn1Al-nitrate. The 7Cu2Zn1Al-nitrate having more copper content does not provide high

activity. CO conversion and DME yield of the 7Cu2Zn1Al-ntirate were lower than for the 5Cu4Zn1Al-nitrate. The selectivity, however, was not influenced much from Cu/Zn ratio. It can be concluded that copper and zinc have its optimal ratio in the 6Cu3Zn1Al-nitrate sample. This well agreed with the former research that copper cannot be solely responsible for high activity [24]. Zinc oxides should interact with copper defect sites as well as there should be enough accessible copper surface area. In addition, the activity is not exclusively related to the reduction temperature for FSP catalysts.

We have finally investigated the 6Cu3Zn1Al-nitrate catalyst further. Figure 12 shows the conversion and selectivity with various pressures and GHSVs. Decreasing of the reaction pressure reduced the conversion of CO. This is due to the fact that the thermodynamic equilibrium of methanol synthesis and consequently that of direct DME synthesis are lowered at decreasing pressure [8]. DME selectivity was not influenced by the reaction pressure except for 215 ^{o}C. At low temperature and low pressure condition, methanol synthesis reaction might be more favorable than water gas shift. Therefore, more methanol than CO_2 has been produced and the methanol subsequently has been converted to DME. As shown in Figure 12 (c), the CO conversion decreases with increase of GHSV. Nevertheless, the DME selectivity was constant. Methanol synthesis was restricted by pressure and GHSV, while methanol dehydration was not. Therefore, the development of methanol synthesis catalysts is crucial in order to increase the overall DME yield in direct DME synthesis.

Figure. 12 here

4. Conclusion

Flame spray pyrolysis was demonstrated to achieve fast and simple CZA nanoparticle synthesis. Nitrate-based metal precursors could lead to catalysts having a higher copper surface area and activity in direct DME synthesis than catalysts prepared from organometallic precursors depending on the flame conditions. Comparing with the conventional synthesis method such as co-precipitation, flame spray pyrolysis of nitrate-based precursor solutions could be industrially applicable due to reproducible catalyst preparation with high production rate, little chemical waste, and tolerable cost. Although organometallic precursors have been favored in literature for flame spray pyrolysis to obtain higher surface area, in our study it was verified that nitrate metal precursors – cheaper and less toxic – lead to good CZA catalysts. This study also showed the same effect of the precursor selection on particle surface area. However, in the case of CZA catalysts obtaining a high copper surface area is required to achieve a high catalytic activity. The copper surface area seems to be more influential factor than the BET surface area. This study showed that nitrate-based precursors can be used to prepare catalysts with higher copper surface area. It means that the selection of precursors influences the number of active sites. Consequently, the CZA catalyst synthesized from nitrate precursors has a higher number of active copper sites, which are linked to high activity for

direct DME synthesis. At the high temperature condition, the catalytic performance of 6Cu3Zn1Al-nitrate catalyst was the same as the commercial catalyst. The final DME selectivity shows less correlation with the activity of CZA. All the catalyst presented a similar DME selectivity. On the other hand, the Cu/Zn ratio influenced the catalytic activity. The ratio 2 is close to the optimum ratio.

Acknowledgement

The support of the Helmholtz Research School on Energy-Related Catalysis is gratefully acknowledged. We would like to appreciate to Dr.-Ing. H. Störmer for TEM measurements and PrivDoz. Dr. habil. S. Behrens and Ms. S. Essig for XRD measurements.

References

[1] I. Sierra, J. Erena, A.T. Aguayo, M. Olazar, J. Bilbao, Deactivation kinetics for direct dimethyl ether synthesis on a CuO-ZnO-Al_2O_3/γ-Al_2O_3 catalyst, Ind. Eng. Chem. Res., 49 (2010) 481-489.

[2] J.Q. Chen, A. Bozzano, B. Glover, T. Fuglerud, S. Kvisle, Recent advancements in ethylene and propylene production using the UOP/Hydro MTO process, Catal. Today, 106 (2005) 103-107.

[3] P. Cheung, A. Bhan, G.J. Sunley, D.J. Law, E. Iglesia, Site requirements and elementary steps in dimethyl ether carbonylation catalyzed by acidic zeolites, J. Catal., 245 (2007) 110-123.

[4] A.T. Aguayo, J. Erena, D. Mier, J.M. Arandes, M. Olazar, J. Bilbao, Kinetic modeling of dimethyl ether synthesis in a single step on a CuO-ZnO-Al_2O_3/γ-Al_2O_3 catalyst, Ind. Eng. Chem. Res., 46 (2007) 5522-5530.

[5] G.R. Moradi, J. Ahmadpour, F. Yaripour, W. J., Equilibrium calculations for direct synthesis of dimethyl ether from syngas, Can. J. Chem. Eng., 89 (2010) 108-115.

[6] J. Yoshihara, S.C. Parker, A. Schafer, C.T. Campbell, Methanol synthesis and reverse water-gas shift kinetics over clean polycrystalline copper, Catal. Lett., 31 (1995) 313-324.

[7] J.T. Sun, I.S. Metcalfe, M. Sahibzada, Deactivation of Cu/ZnO/Al_2O_3 methanol synthesis catalyst by sintering, Ind. Eng. Chem. Res., 38 (1999) 3868-3872.

[8] J.B. Hansen, P.E.H. Nielsen, Methanol synthesis, in: G. Ertl, H. Knözinger, F. Schüth, J. Weitkamp (Eds.) Handbook of heterogeneous catalysis, Wiley-VCH Verlag GmbH & Co. KGaA., 2008, pp. 2920-2949.

[9] M. Behrens, F. Studt, I. Kasatkin, S. Kuhl, M. Havecker, F. Abild-Pedersen, S. Zander, F. Girgsdies, P. Kurr, B.L. Kniep, M. Tovar, R.W. Fischer, J.K. Nørskov, R. Schlögl, The active site of methanol synthesis over Cu/ZnO/Al_2O_3 industrial catalysts, Science, 336 (2012) 893-897.

[10] M. Behrens, S. Zander, P. Kurr, N. Jacobsen, J. Senker, G. Koch, T. Ressler, R.W. Fischer, R. Schlögl, Performance improvement of nanocatalysts by promoter-induced defects in the support material: methanol synthesis over Cu/ZnO:Al, J. Am. Chem. Soc., 135 (2013) 6061-6068.

[11] C. Baltes, S. Vukojevic, F. Schüth, Correlations between synthesis, precursor, and catalyst structure and activity of a large set of $CuO/ZnO/Al_2O_3$ catalysts for methanol synthesis, J. Catal., 258 (2008) 334-344.

[12] R. Jossen, Controlled synthesis of mixed oxide nanoparticles by flame spray pyrolysis, PhD Thesis, Swiss Federal Institute of Technology Zurich.

[13] H.K. Kammler, L. Mädler, S.E. Pratsinis, Flame synthesis of nanoparticles, Chem. Eng. Technol., 24 (2001) 583-596.

[14] W.Y. Teoh, R. Amal, L. Mädler, Flame spray pyrolysis: An enabling technology for nanoparticles design and fabrication, Nanoscale, 2 (2010) 1324-1347.

[15] J.R. Jensen, T. Johannessen, S. Wedel, H. Livbjerg, A study of $Cu/ZnO/Al_2O_3$ methanol catalysts prepared by flame combustion synthesis, J. Catal., 218 (2003) 67-77.

[16] F. Huber, H. Meland, M. Ronning, H. Venvik, A. Holmen, Comparison of Cu-Ce-Zr and Cu-Zn-Al mixed oxide catalysts for water-gas shift, Top. Catal., 45 (2007) 101-104.

[17] R. Ahmad, M. Hellinger, M. Buchholz, H. Sezen, L. Gharnati, C. Wöll, J. Sauer, M. Döring, J. Grunwaldt, U. Arnold, Flame-made $Cu/ZnO/Al_2O_3$ catalyst for dimethyl ether production, Catal. Commun., 43 (2014) 52-56.

[18] R. Kam, C. Selomulya, R. Amal, J. Scott, The influence of La-doping on the activity and stability of Cu/ZnO catalyst for the low-temperature water-gas shift reaction, J. Catal., 273 (2010) 73-81.

[19] G.C. Chinchen, C.M. Hay, H.D. Vandervell, K.C. Waugh, The measurement of copper surface-areas by reactive frontal chromatography, J. Catal., 103 (1987) 79-86.

[20] Z.Y. Fei, P. Lu, X.Z. Feng, B. Sun, W.J. Ji, Geometrical effect of CuO nanostructures on catalytic benzene combustion, Catal. Sci. Technol., 2 (2012) 1705-1710.

[21] W.P. Dow, Y.P. Wang, T.J. Huang, TPR and XRD studies of yttria-doped ceria/γ-alumina-supported copper oxide catalyst, Appl. Catal. A-Gen., 190 (2000) 25-34.

[22] M. Stiefel, R. Ahmad, U. Arnold, M. Doring, Direct synthesis of dimethyl ether from carbon-monoxide-rich synthesis gas: Influence of dehydration catalysts and operating conditions, Fuel Process. Technol., 92 (2011) 1466-1474.

[23] S. Jiang, J.S. Hwang, T.H. Jin, T.X. Cai, W. Cho, Y.S. Baek, S.E. Park, Dehydration of methanol to dimethyl ether over ZSM-5 zeolite, Bull. Korean Chem. Soc., 25 (2004) 185-189.

[24] S. Zander, E.L. Kunkes, M.E. Schuster, J. Schumann, G. Weinberg, D. Teschner, N. Jacobsen, R. Schlögl, M. Behrens, The Role of the Oxide Component in the Development of Copper Composite Catalysts for Methanol Synthesis, Angew. Chem. Int. Edit., 52 (2013) 6536-6540.

Highlights

- $Cu/ZnO/Al_2O_3$ from water containing nitrate precursors was well synthesized by flame spray pyrolysis.
- The catalyst synthesized form nitrate precursor has higher active surface area than the one from organometallic precursor.
- The direct DME synthesis from syngas was well carried out by using the FSP synthesized catalyst.

Keywords

Flame spray pyrolysis; $Cu/ZnO/Al_2O_3$; H-ZSM-5; Direct DME synthesis; Syngas

Table 1. Surface area, copper surface area and CuO content

	BET surface area (m^2/g_{cat})	Cu surface area (m^2/g_{cat})[1)]	N_2O chemisorption capacity ($\mu mol/g_{cat}$)	CuO (wt. %)[2)]
5Cu4Zn1Al-nitrate	33.39	13.8	170	-
6Cu3Zn1Al-nitrate	41.04	18.6	226	63.4
7Cu2Zn1Al-nitrate	39.95	16.4	200	-
5Cu4Zn1Al-organo	54.00	8.6	104	-
6Cu3Zn1Al-organo	63.70	10.6	130	55.1
7Cu2Zn1Al-organo	60.77	7.0	86	-

[1)] Determined by N_2O-RFC. [2)] Amount of CuO was measured based on TPR before the N_2O chemisorption analysis.

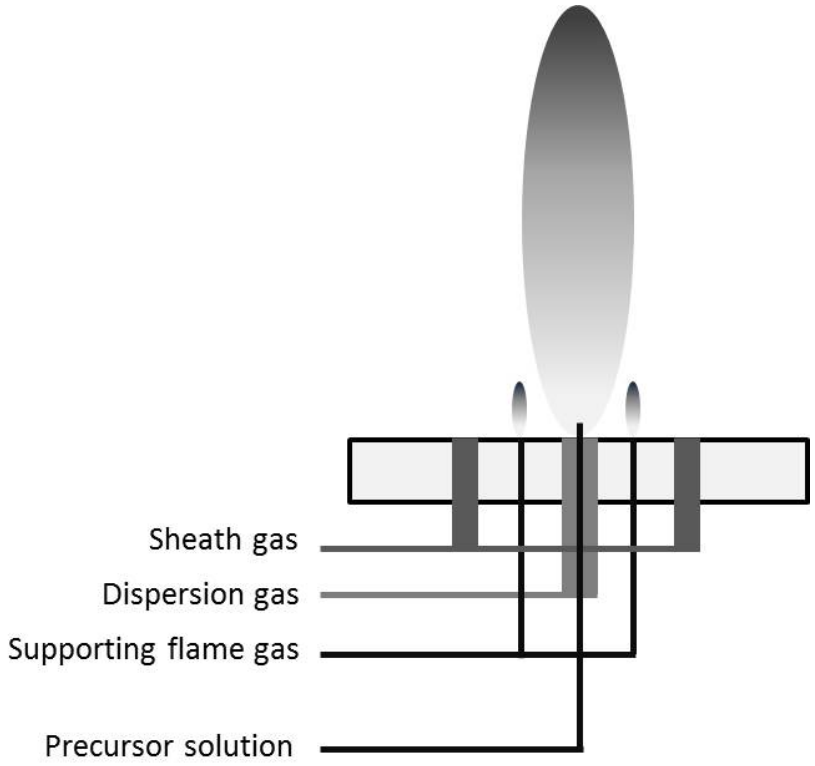

Figure 1. Scheme of a flame generator.

Figure 2. The flame pictures of 6Cu3Zn1Al-nitrate (a) and 6Cu3Zn1Al-organo (b).

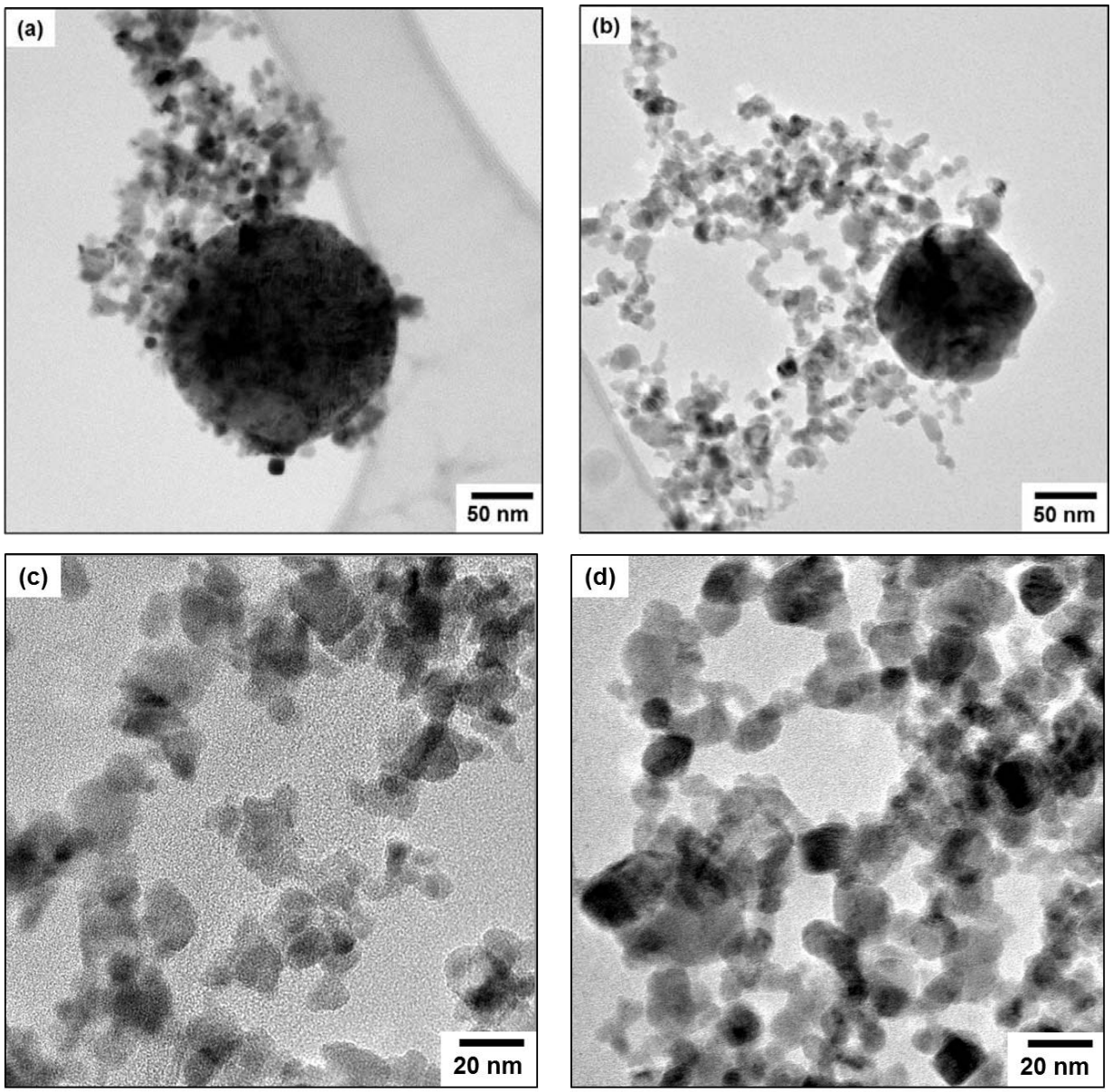

Figure 3. TEM images of FSP synthesized CZA: 6Cu3Zn1Al-nitrate (a, c), 6Cu3Zn1Al-organo (b, d).

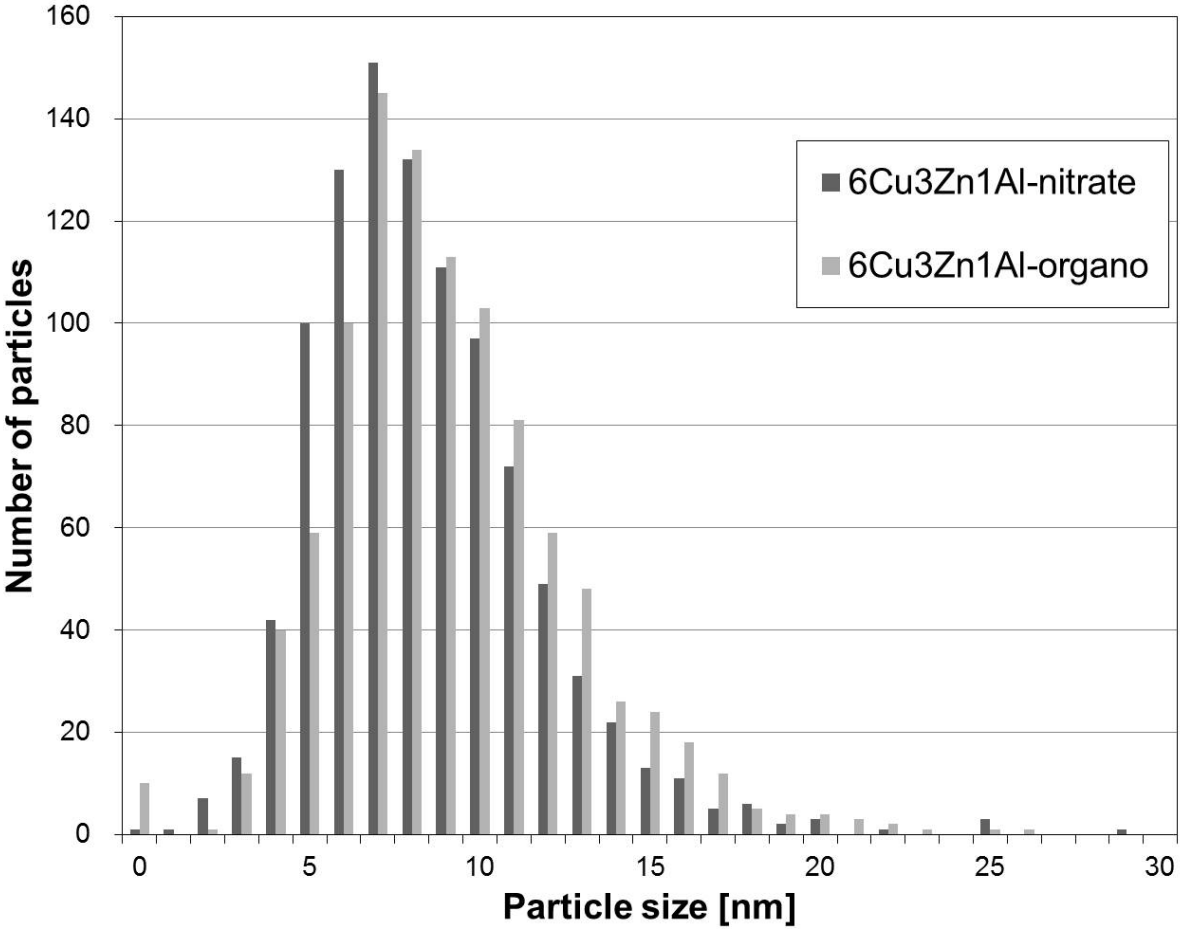

Figure 4. Particle size distribution of 6Cu3Zn1Al-nitrate and 6Cu3Zn1Al-organo.

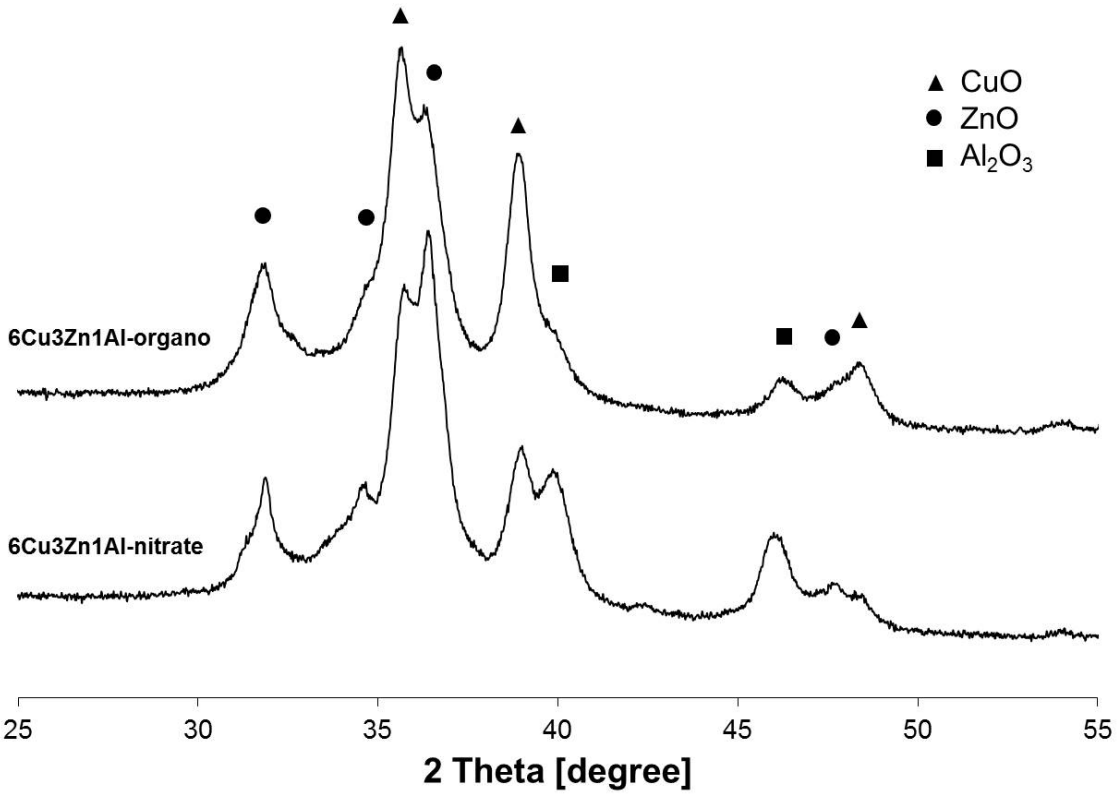

Figure 5. XRD patterns of 6Cu3Zn1Al-nitrate and 6Cu3Zn1Al-organo.

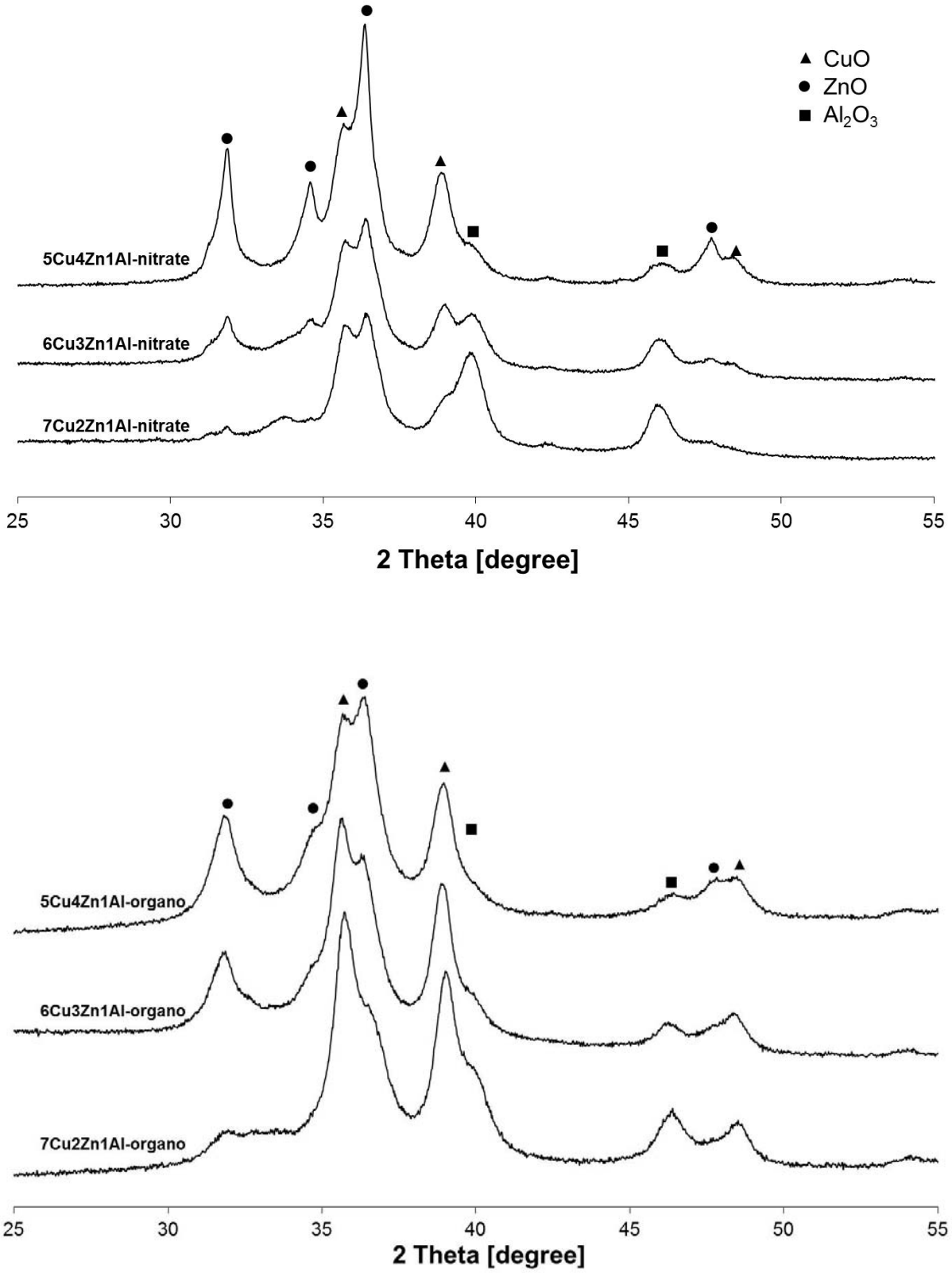

Figure 6. XRD patterns of the nitrate type and organometallic type.

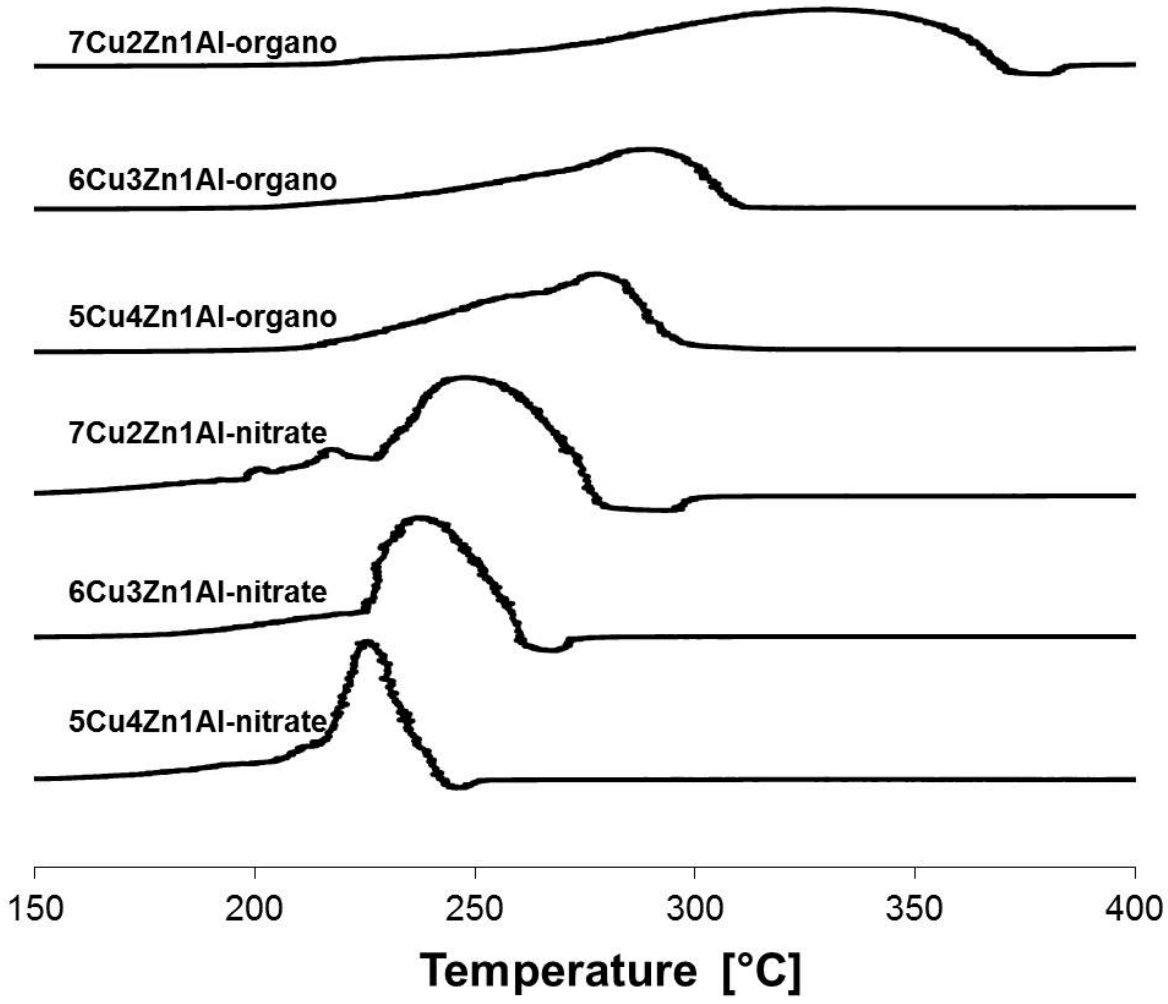

Figure 7. TPR spectra of the nitrate type and organometallic type.

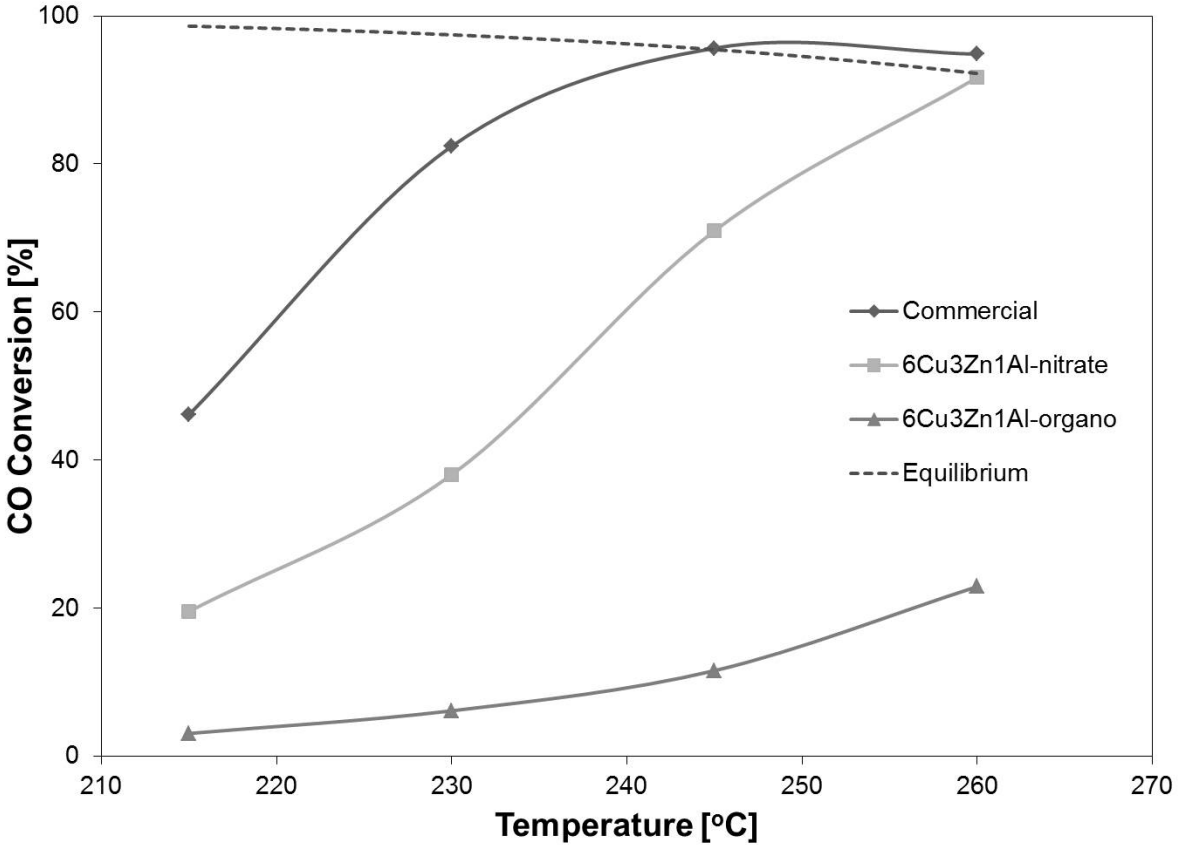

Figure 8. CO conversion of the commercial CZA catalyst, 6Cu3Zn1Al-nitrate and 6Cu3Zn1Al-organo as a function of temperature. GHSV = 900 $Nml \cdot h^{-1} \cdot g_{cat}^{-1}$, 40 bar.

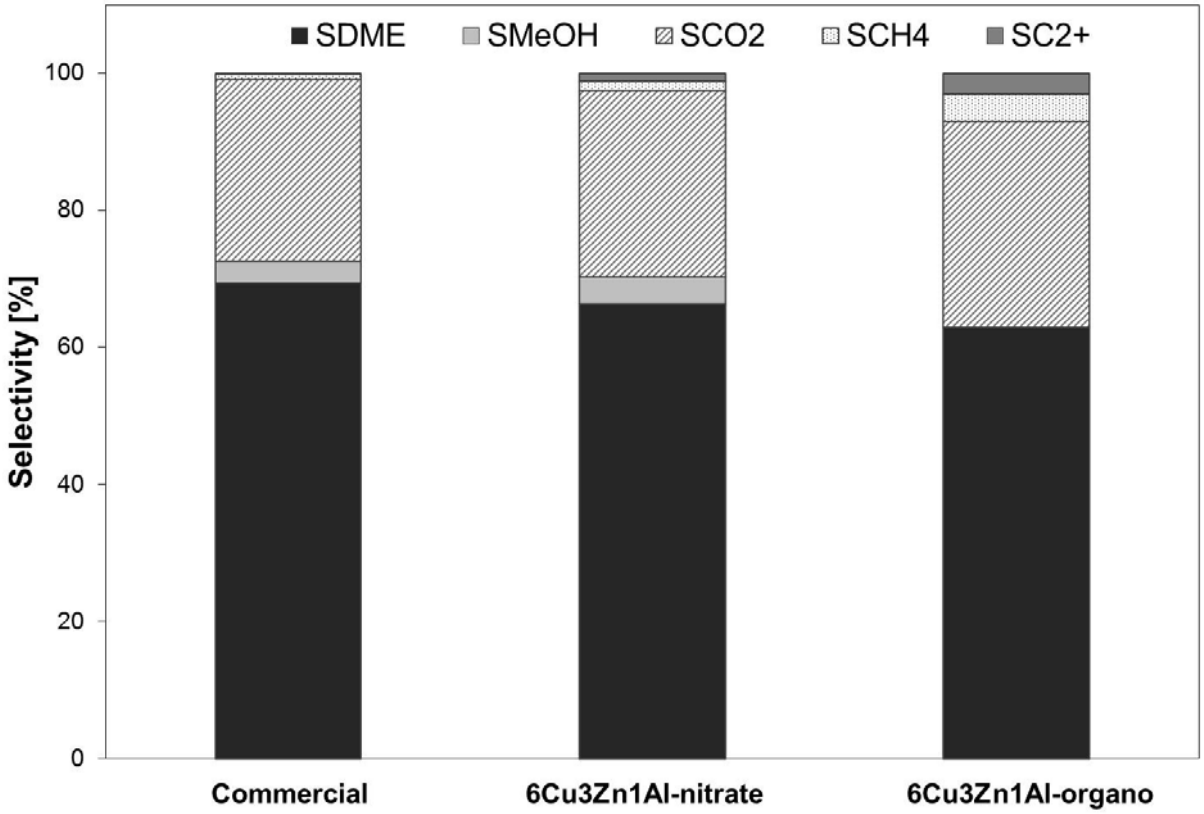

Figure 9. Selectivity of the commercial CZA catalyst, 6Cu3Zn1Al-nitrate and 6Cu3Zn1Al-organo. GHSV = 900 $Nml \cdot h^{-1} \cdot g_{cat}^{-1}$, 40 bar, 260 ^{o}C.

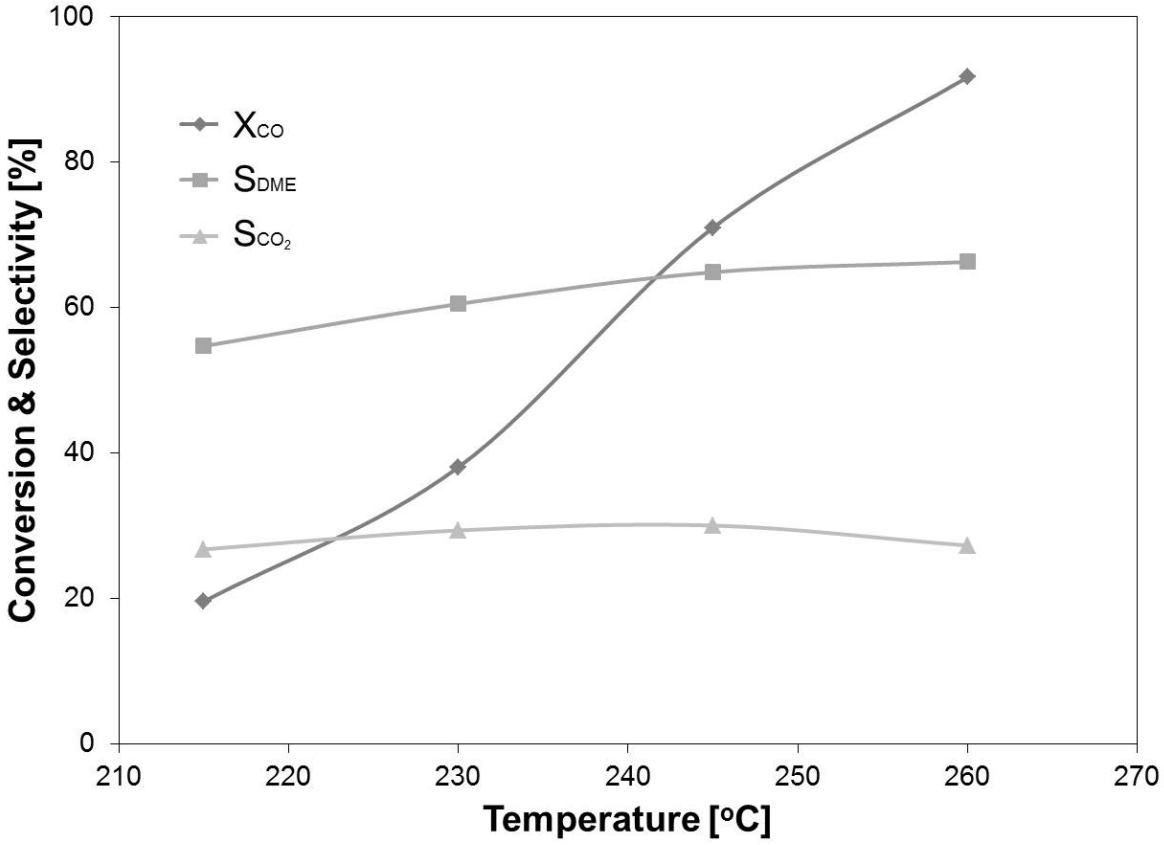

Figure 10. CO conversion and DME and CO_2 selectivity of 6Cu3Zn1Al-nitrate as a function of temperature. GHSV = 900 $Nml \cdot h^{-1} \cdot g_{cat}^{-1}$, 40 bar.

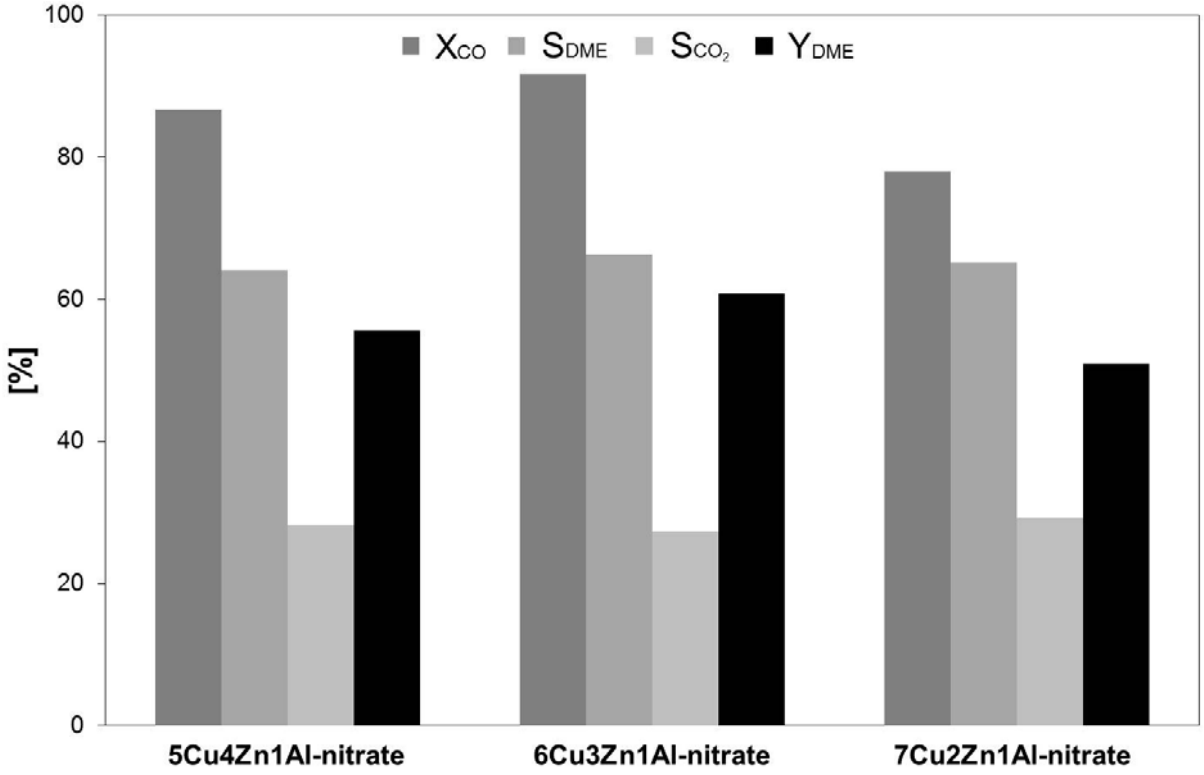

Figure 11. CO conversion and DME and CO_2 selectivity of the nitrate type catalysts. GHSV = 900 Nml·h^{-1}·g_{cat}^{-1}, 40 bar, 260 ^{o}C.

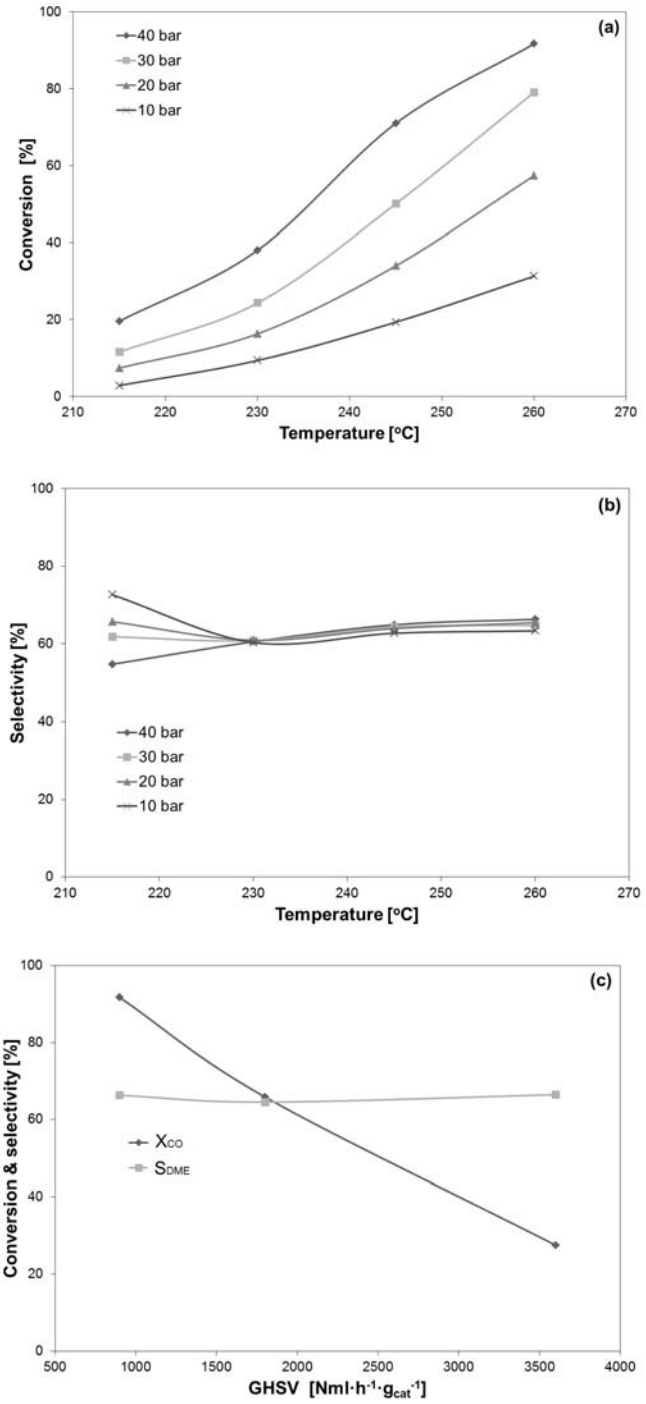

Figure 12. Pressure effect in the direct DME synthesis over 6Cu3Zn1Al-nitrate: CO conversion (a) and DME selectivity (b) as a function of temperature; GHSV = 900 $Nml \cdot h^{-1} \cdot g_{cat}^{-1}$. CO conversion and DME selectivity of 6Cu3Zn1Al-nitrate as a function of GHSV (c); 40 bar, 260 ^{o}C.